

Thermoelectric Properties of Self Assembled $\text{TiO}_2/\text{SnO}_2$ Nanocomposites

Fred Dynys*, NASA Glenn, USA;

Ali Sayir, Alp Sehirlioglu, Case Western Reserve University, USA

Recent advances in improving efficiency of thermoelectric materials are linked to nanotechnology. Thermodynamically driven spinodal decomposition was utilized to synthesize bulk nanocomposites. $\text{TiO}_2/\text{SnO}_2$ system exhibits a large spinodal region, ranging from 15 to 85 mole % TiO_2 . The phase separated microstructures are stable up to 1400 °C. Semiconducting $\text{TiO}_2/\text{SnO}_2$ powders were synthesized by solid state reaction between TiO_2 and SnO_2 . High density samples were fabricated by pressureless sintering. Self assemble nanocomposites were achieved by annealing at 1000 to 1350 °C. X-ray diffraction reveal phase separation of $(\text{Ti}_x\text{Sn}_{1-x})\text{O}_2$ type phases. The $\text{TiO}_2/\text{SnO}_2$ nanocomposites exhibit n-type behavior; a power factor of 70 W/mK^2 at 1000 °C has been achieved with penta-valent doping. Seebeck, thermal conductivity, electrical resistivity and microstructure will be discussed in relation to composition and doping.



Thermoelectric Properties of Self Assembled $\text{TiO}_2/\text{SnO}_2$ Nanocomposites

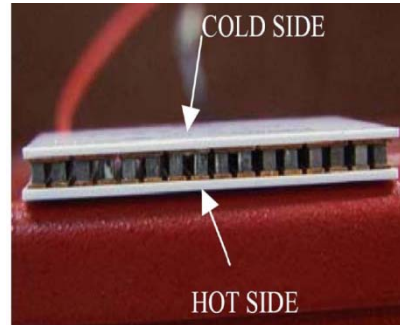
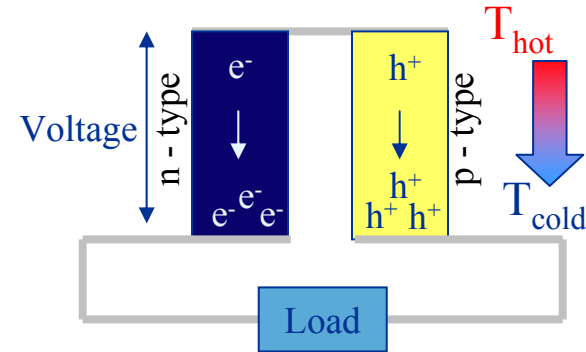
Fred Dynys, NASA-Glenn, USA

Ali Sayir, CWRU, USA

Alp Sehirlioglu, CWRU, USA

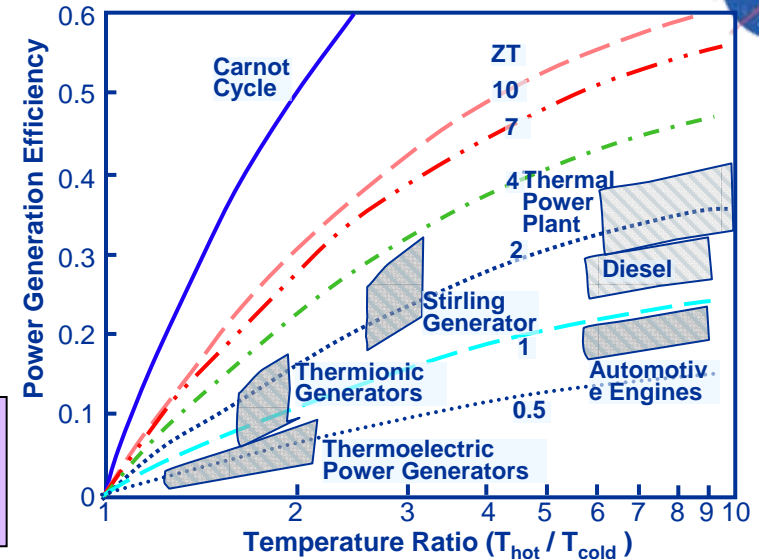
Program Support: NASA Radioisotope Power Systems

Heat to Electric Power Generation

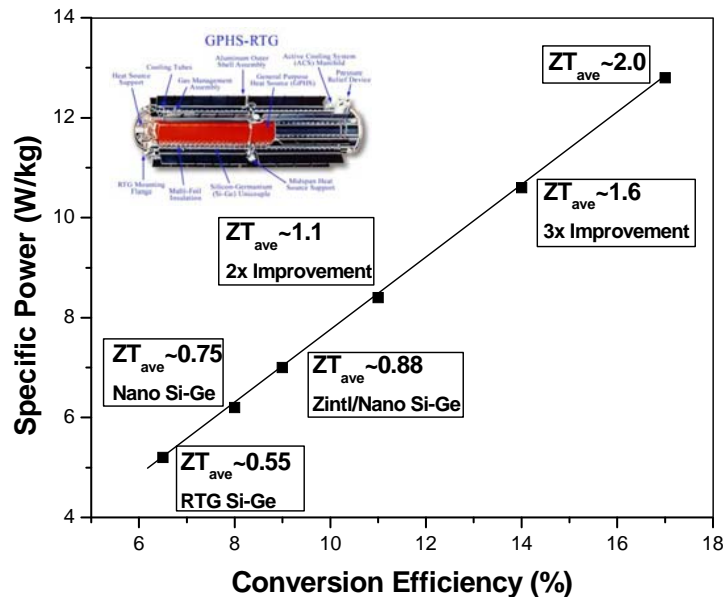


Objective: High Conversion Efficiency

- Reduces Mass, Volume & Cost



Space Power Generation



Waste Heat to Power

- Waste Heat is one of our most under utilized energy resources
- U.S.-energy consumption ~ 29 tera-kWh (10^{12}) Barrels of Oil – 170 giga-barrels (10^9)
- World-energy consumption ~ 120 tera- kWh (10^{12})
- 20-65 percent is lost in the form of heat
- Maximizes efficiency
- Reduces CO_2 emission

Figure of Merit

$$ZT = \frac{S^2 \sigma}{\kappa} T$$

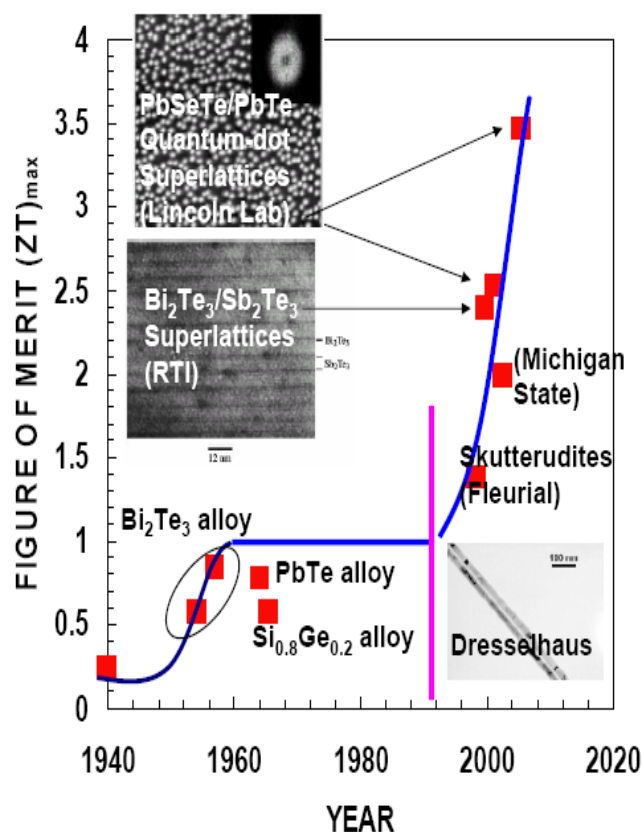
S - Seebeck coefficient
 σ - electrical conductivity
 κ - thermal conductivity

Efficiency

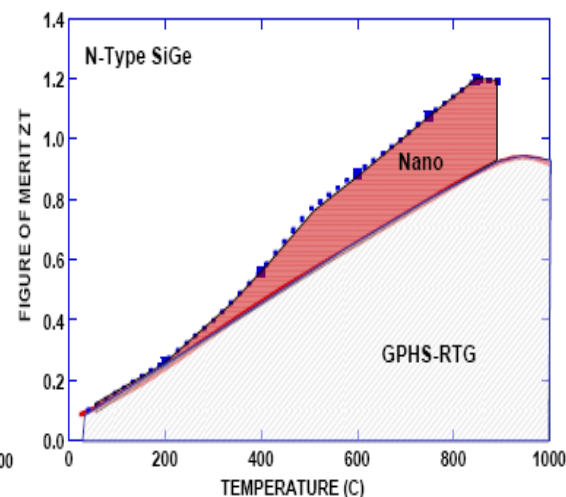
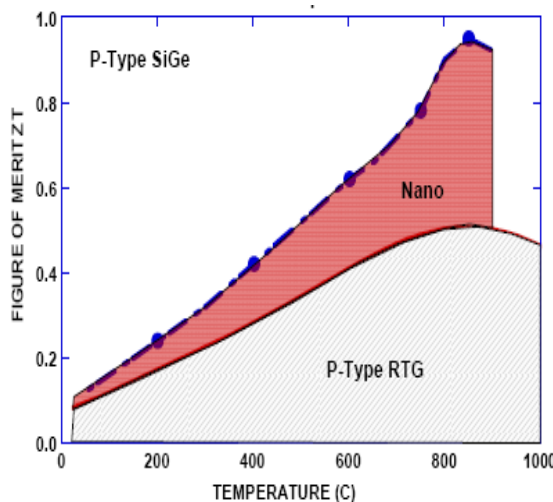
$$\eta_{\max} = \frac{\Delta T}{T_{\text{hot}}} \frac{\sqrt{1 + ZT} - 1}{\sqrt{1 + ZT} + T_{\text{cold}}/T_{\text{hot}}}$$

Phonon Scattering:

- Atom disorder
- Alloying
- Anharmonic vibrations
- Supperlattices
- Crystal Structures
- Nano-technology



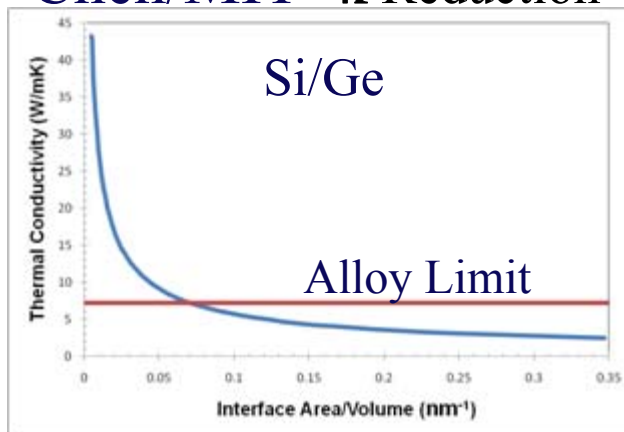
Fleurial/Chen – JPL/MIT



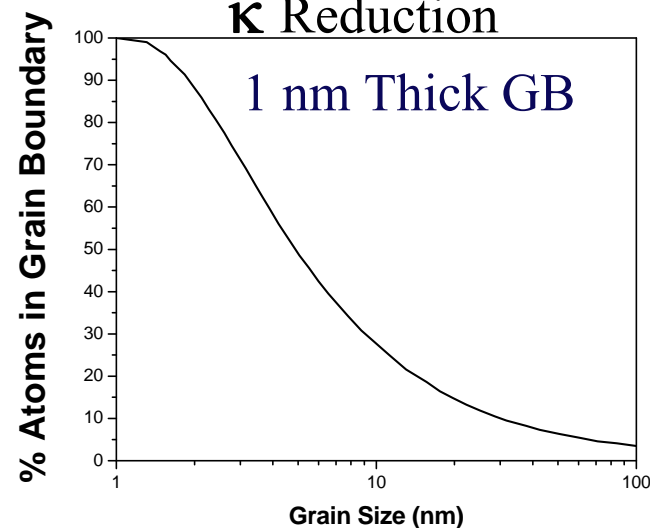
Fabrication of Nanostructure Solids

Goal: Preservation of the nanostructure during fabrication.

Chen/MIT- κ Reduction



κ Reduction



**Nano-powder
Synthesis**

**Thermal
Densification**
Pressure Assisted
Microwave
Laser
Plasma-SPS/P²C

**Cold
Densification**
Cold Spray
Dynamic Compaction
Plastic Deformation

Inhibit Grain Growth

- Rapid Thermal Process
- Inclusions

**Post
Process**

~~Nano-Powder~~

Thermodynamics
Phase Transformation
Precipitation
Spinodal Decomposition

- Microstructure
Dependent on Thermal
Aging
- Composition Limited

Spinodal Decomposition

TiO₂ – SnO₂

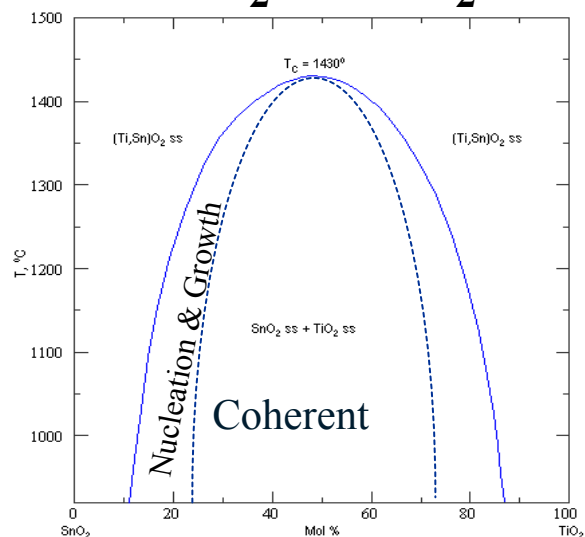


Fig. 10. TEM image of (Ti_{0.5}/Sn_{0.5})O₂ ceramics annealed for 48 h.

Desired Features

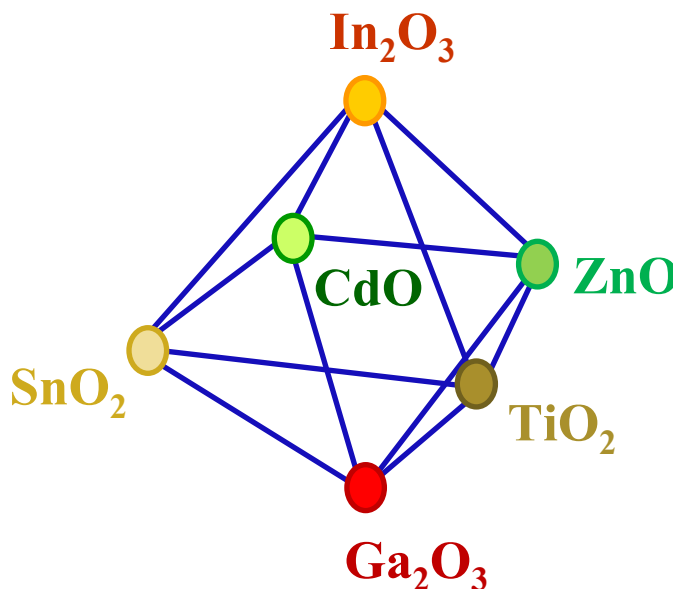
- ~50 nm grains
- High Temperature
- Wide Composition
- Large Δ Mass

Transparent Conducting Oxides

- Large Bandgap 2.4-3.8 eV
- N-type – Degenerate Semiconductor

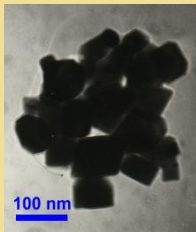
Electrical Conductivity

TCO	σ (S/m) @ RT
ITO	8×10^5
In ₂ O ₃	1×10^6
SnO ₂	2.5×10^5
ZnO	8.3×10^5
ZnO:Al	7.7×10^4
CdSnO ₂	7.7×10^5
CdO:In	1.7×10^6
TiO ₂	0.01

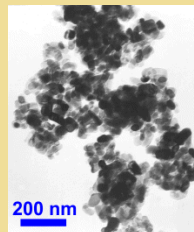


ZnO:Al
ZT=0.3 @ 1000 °C

SnO_2
Purity: 99.9%
APS: 50 nm
SSA: $14.2 \text{ m}^2/\text{g}$



TiO_2 Rutile
Purity: 99.99 %
APS: 20 nm,
SSA: $> 30 \text{ m}^2/\text{g}$



Dopants
 CoO , MnO
 Ta_2O_5 , In_2O_3

$\text{TiO}_2/\text{SnO}_2$
50/50 mol %
75/25 mol %
25/75 mol %

Powder
Mixing

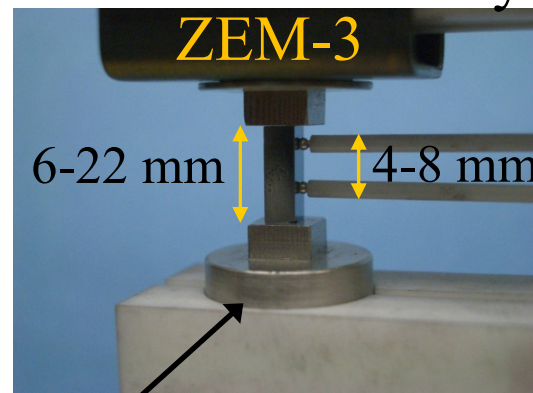
Compaction
Die Press

Reactive Sintering
1250-1550 °C

Thermal Conductivity

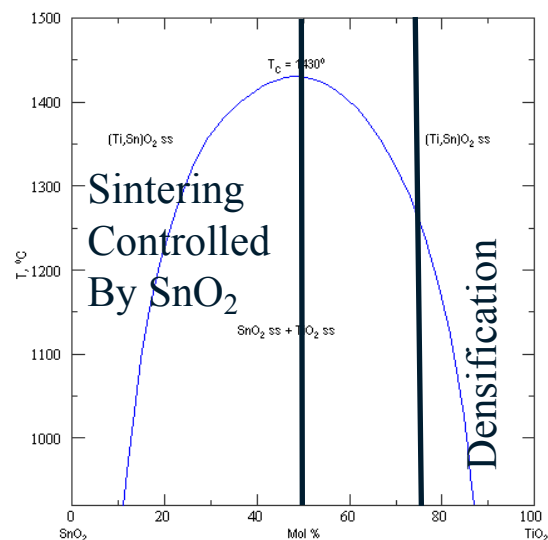
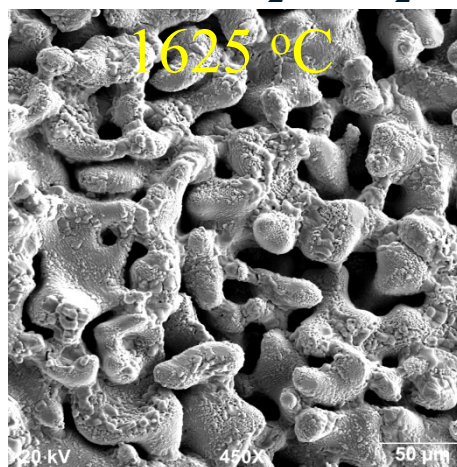
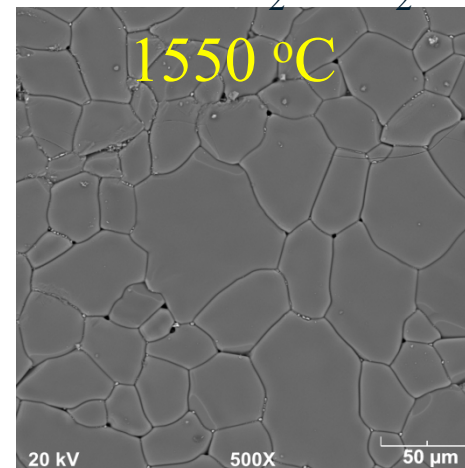
- Laser Flash Method- Thermal Diffusivity
- Standard
- Specific Heat-Laser Flash
- Thermal Conductivity ($K = \alpha \rho C_p$)

Seebeck/Resistivity



ΔT 0-50 °C/Furnace RT-1000 °C

Sintering

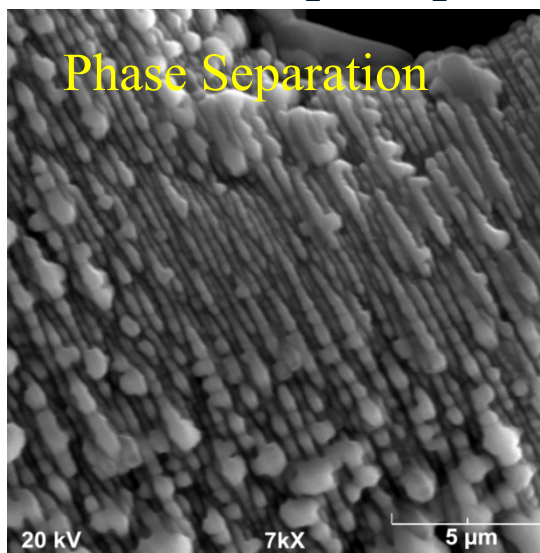
50/50 $\text{TiO}_2/\text{SnO}_2$ 75/25 $\text{TiO}_2/\text{SnO}_2$ 

Sintering-Inhibited

- Surface Diffusion $< 1100^\circ\text{C}$
 - Evaporation $> 1100^\circ\text{C}$
- $$\text{SnO}_2 \rightarrow \text{SnO} + \frac{1}{2}\text{O}_2(\text{g})$$

Sintering Aids

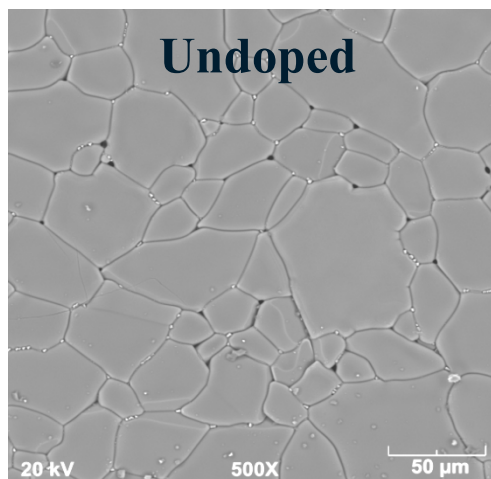
- MnO , CoO , CuO , ZnO

50/50 $\text{TiO}_2/\text{SnO}_2$ 

Ta_2O_5 & In_2O_3
Ineffective Sintering Aids

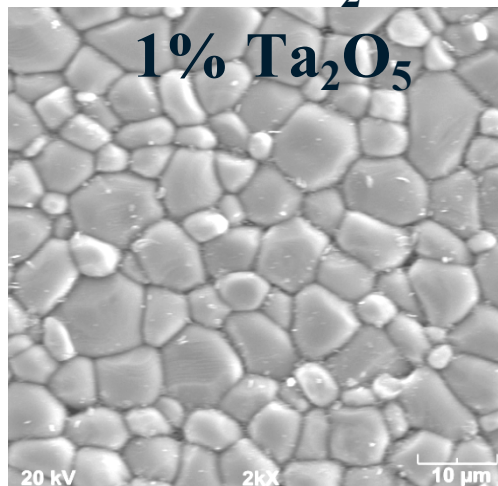


75/25 $\text{TiO}_2/\text{SnO}_2$



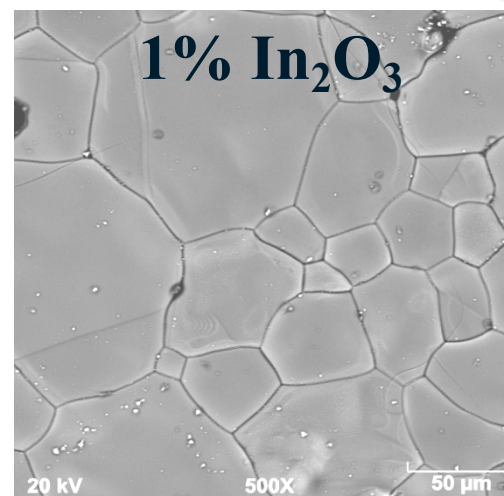
XRD-Phases

Sintered – $(\text{Ti}_{0.8}\text{Sn}_{0.2})\text{O}_2$
 Reduced – TiO_2 , Rutile
 $(\text{Ti}_{0.8}\text{Sn}_{0.2})\text{O}_2$



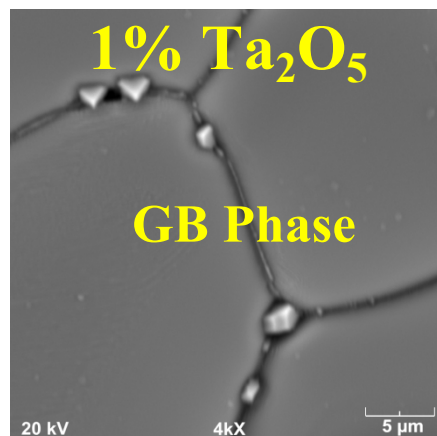
XRD-Phases

Sintered – $(\text{Ti}_{0.8}\text{Sn}_{0.2})\text{O}_2$
 Annealed – $(\text{Ti}_{0.8}\text{Sn}_{0.2})\text{O}_2$
 1250 °C
 Reduced – TiO_2 , Rutile
 $(\text{Ti}_{0.8}\text{Sn}_{0.2})\text{O}_2$



XRD-Phases

Sintered – TiO_2 , Rutile
 SnO_2 , In_2O_3
 Annealed – TiO_2 , Rutile
 1250 °C SnO_2 , In_2O_3



Phase Separation

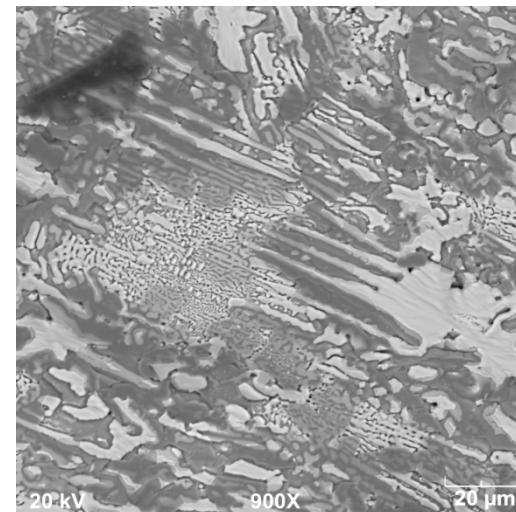
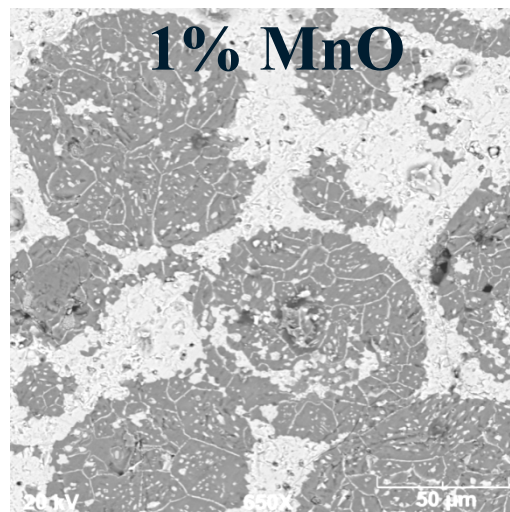
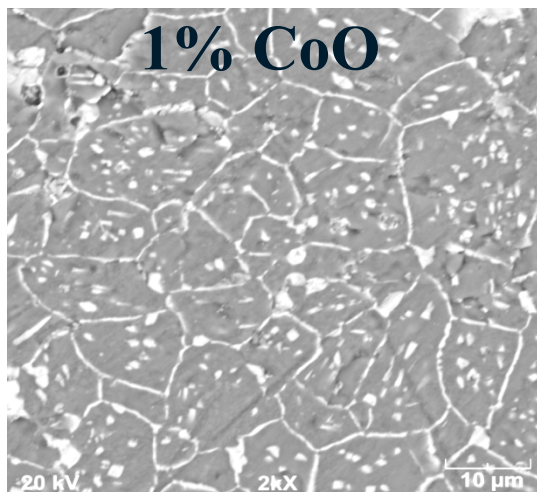
1% CoO XRD

Sintered – $(\text{Ti}_{0.8}\text{Sn}_{0.2})\text{O}_2$
 $(\text{Ti}_{0.2}\text{Sn}_{0.8})\text{O}_2$
 Annealed – $(\text{Ti}_{0.9}\text{Sn}_{0.1})\text{O}_2$
 1000 °C $(\text{Ti}_{0.1}\text{Sn}_{0.9})\text{O}_2$

1% MnO XRD

Sintered – $(\text{Ti}_{0.8}\text{Sn}_{0.2})\text{O}_2$
 $(\text{Ti}_{0.2}\text{Sn}_{0.8})\text{O}_2$
 Annealed – $(\text{Ti}_{0.9}\text{Sn}_{0.1})\text{O}_2$
 1000 °C $(\text{Ti}_{0.1}\text{Sn}_{0.9})\text{O}_2$

50/50 $\text{TiO}_2/\text{SnO}_2$



XRD-Phases

Sintered – $(\text{Ti}_{0.8}\text{Sn}_{0.2})\text{O}_2$
 $(\text{Ti}_{0.2}\text{Sn}_{0.8})\text{O}_2$
 TiO_2
 Annealed – $(\text{Ti}_{0.2}\text{Sn}_{0.8})\text{O}_2$
 1000 °C $(\text{Ti}_{0.9}\text{Sn}_{0.1})\text{O}_2$

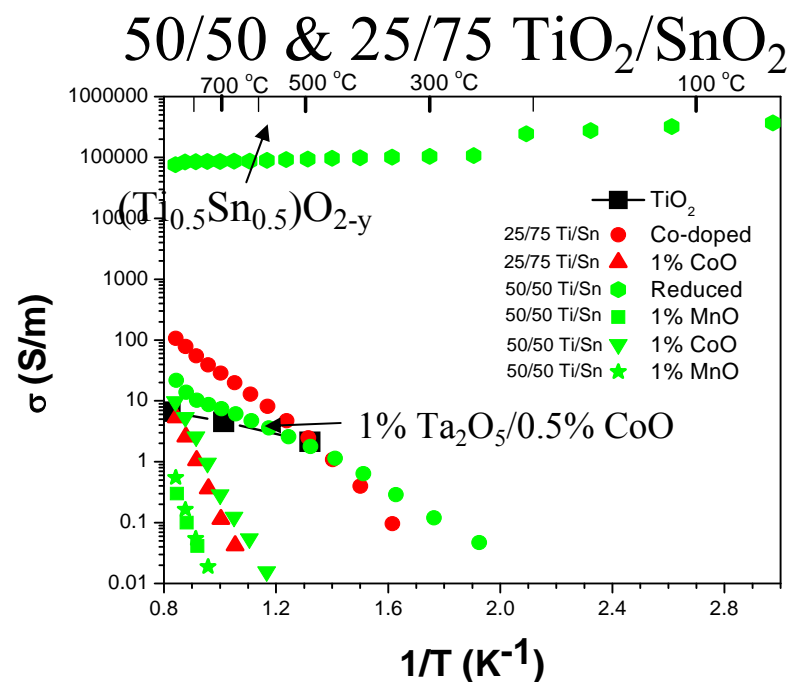
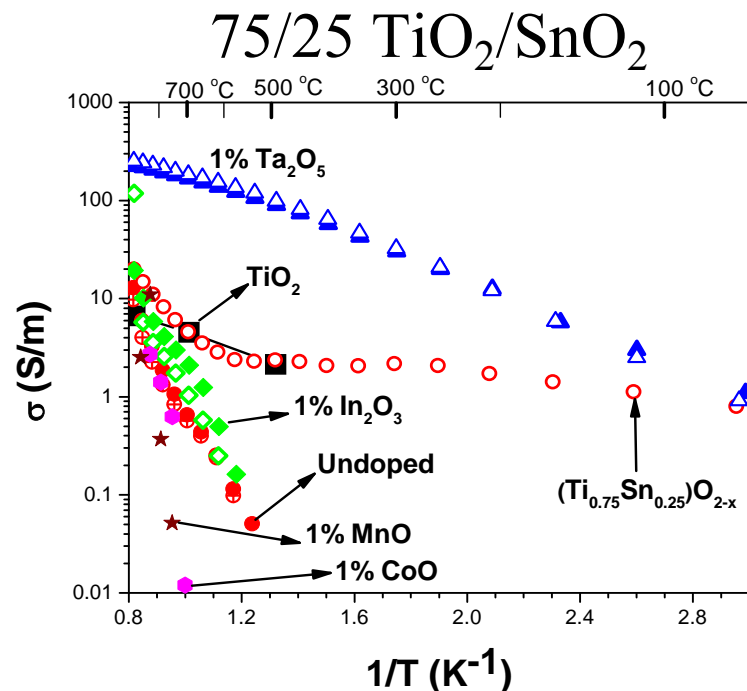
XRD-Phases

Sintered – $(\text{Ti}_{0.8}\text{Sn}_{0.2})\text{O}_2$
 $(\text{Ti}_{0.1}\text{Sn}_{0.9})\text{O}_2$
 Annealed – $(\text{Ti}_{0.2}\text{Sn}_{0.8})\text{O}_2$
 1000 °C $(\text{Ti}_{0.9}\text{Sn}_{0.1})\text{O}_2$

Microstructure
 Coarsening
 @ 1600 °C

Grain Boundary Phases
 Segregation

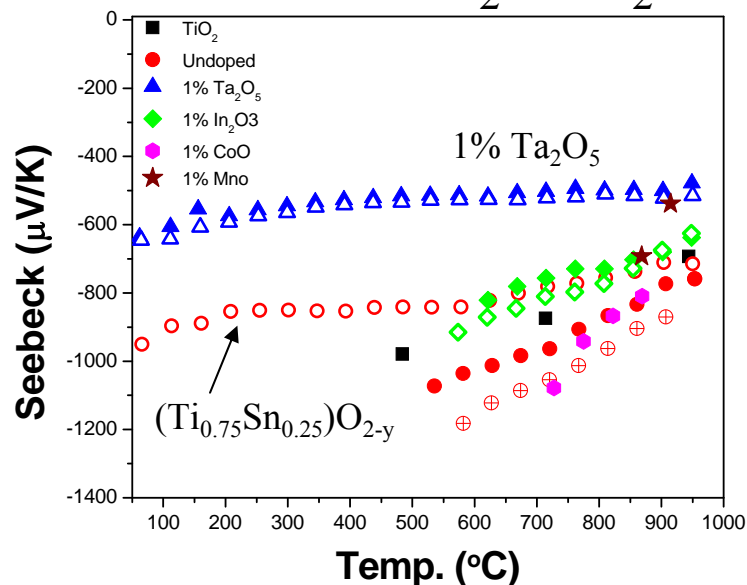
Electrical Conductivity



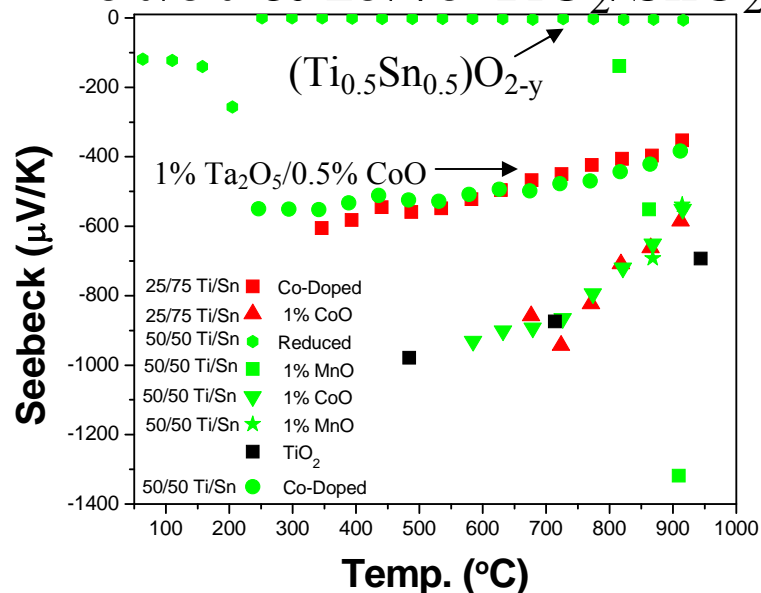
- Ta₂O₅ – Increases σ – $E_a \sim 0.25$ eV
- (Ti_xSn_{1-x})O_{2-y} – Oxygen Deficiency Increases σ – $E_a \sim 0.06$ eV
- Co-doping-Ta₂O₅/CoO - Increases σ – $E_a \sim 0.5-0.7$ eV
- In₂O₃, MnO & CoO – Ineffective in Enhancing σ – $E_a \sim 1-4.2$ eV

Seebeck Coefficient

75/25 $\text{TiO}_2/\text{SnO}_2$

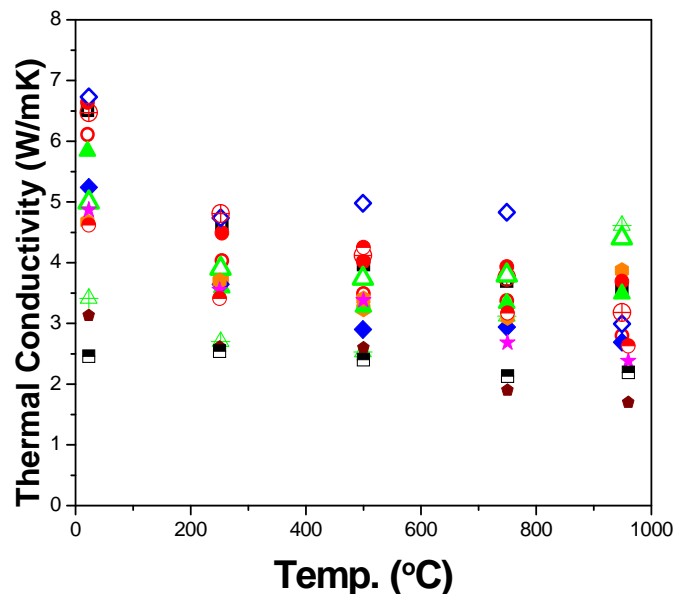
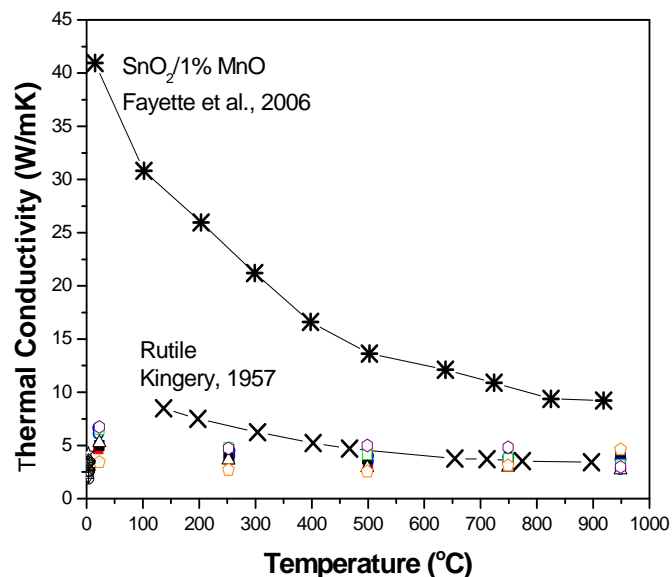


50/50 & 25/75 $\text{TiO}_2/\text{SnO}_2$



- N-type
- Large Seebeck coefficients $> -400 \mu\text{V/K}$
- Large Seebeck coefficient – Low σ
- $(\text{Ti}_{0.5}\text{Sn}_{0.5})\text{O}_{2-y}$ low Seebeck ~ 0

Thermal Conductivity



Compositions

1% MnO-50 TiO₂
 1% CoO-50 TiO₂
 1% MnO-75 TiO₂
 1% CoO-75 TiO₂
 1% MnO-25 TiO₂
 1% CoO- 25TiO₂
 1%Ta₂O₅/0.5%
 CoO-25 TiO₂

- Compositions exhibit low κ – 1.7 to 6.8 W/mK
- Observe no dependence on composition or post treatments
- Spinodal Decomposition – κ reduction ?
- Best ZT ~ 0.05



In Summary

- $\text{TiO}_2/\text{SnO}_2$ compositions exhibit low thermal conductivity. Reduction in thermal conductance by spinodal microstructure has not been isolated.
- Improvements in electrical conductivity is needed. Grain boundary phases could be detrimental. Ta_2O_5 or oxygen deficiency enhances electrical conductivity.
- Sintering aids are required to densify equal-molar and tin oxide rich compositions. MnO and CoO promoted phase separation.